Thermochimica Acta, 26 (1978) 383–398

THE THERMAL ANALYSIS OF WAXES AND PETROLATUMS*

HAROLD R. FAUST
Pennzoil Company, Research and Development Department, Shreveport, Louisiana 71106 (U.S.A.)

ABSTRACT

The melting and crystallization characteristics of paraffin waxes and petrolatums were studied using a Perkin-Elmer DSC-1B. Since these materials begin transitions at subambient temperatures, it was necessary to cool with liquid nitrogen in order to obtain stable baselines prior to the onset temperatures. Heats of fusion of waxes and petrolatums were determined by measuring the total endothermic areas. The crystallinities of waxes were determined from experimental heats of fusion and literature values for the pure normal paraffins. The effects of temperature program rate on the peak temperatures of waxes were determined from crystallization and melting scans. The curves were extrapolated to the equilibrium melting point at zero temperature program rate. Specific heat and enthalpy curves were generated from DSC melting curves and "no-sample baselines". Using sapphire as a standard, specific heats were also measured outside of the range where endothermic transitions occurred.

INTRODUCTION

Petroleum waxes are familiar products with applications ranging from candles and crayons to packaging and dentistry. Petrolatum is less familiar but also has wide-ranging applications. Among the most important properties of both waxes and petrolatums are their melting and crystallization characteristics. Inevitably, the first thing a consumer does after receiving a shipment of these materials is to melt them. After processing or blending with other ingredients, the final product is cooled and allowed to crystallize. Numerous investigators have reported on the thermal analysis of paraffin waxes[1–5]. Fewer people have studied petrolatums[6, 7]. Most of the reports show DSC or DTA scans starting around room temperature and programming to higher temperatures. It is the purpose of this investigation to study the melting and crystallization of paraffin wax and petrolatum from subambient temperatures to temperatures above the melting point.

The quantitative measure of heat is important in an energy-conscious society. The amount of heat required to melt 10 or 20 thousand gallons of wax or petrolatum

* Presented at the 7th North American Thermal Analysis Society Conference, St. Louis, Missouri, September 25–28, 1977.

in a railroad car involves a considerable expenditure of energy. Although the handling of waxy materials has been an energy consuming business, the ability of waxes to store heat may conserve energy in the future. Several groups are currently evaluating the use of paraffin waxes as "phase change materials to store solar energy". A further objective of this study is to quantitize heat effects of waxes so that engineering calculations can be made that will lead to optimum energy use.

EXPERIMENTAL

Instrumentation

The work described in this study was performed using a Perkin-Elmer differential scanning calorimeter Model DSC-1B. The sample chamber was continuously purged with dry nitrogen. Liquid nitrogen was used as a coolant in a Perkin-Elmer low temperature cover (Dewar flask). The standard cover was wrapped with additional insulation so that sufficient liquid nitrogen remained during an analysis to cover the sample area. If all of the liquid nitrogen evaporated during a scan, the baseline drifted even though the instrument indicated temperature control.

The use of liquid nitrogen inevitably leads to condensation of moisture in and around the instrument. Therefore, the entire analyzer unit was placed in a Plexiglass dry box which was continuously purged with dry nitrogen[8]. Liquid nitrogen coolant was introduced through a tube connected to the top of the dry box. The boiling nitrogen helped maintain an inert atmosphere inside the box.

The positioning of the aluminum pans on the center of the sample platform is important in DSC work. The slightest movement of the pans or their covers will result in nonreproducible curves. It is critical to avoid any jarring or vibration of the analyzer unit. The use of a polyurethane pad under the unit undoubtedly saved us many frustrating moments. In addition, we found it necessary to avoid using the locking mechanism for the low temperature cover because of its jarring action. Stainless steel plates positioned on top of the cover provided enough pressure to seal the cover over the sample chamber.

Sample preparation

The relatively soft nature of the materials studied necessitated the use of Perkin-Elmer's volatile sample containers. These containers cold weld the aluminum pans to their covers and avoid squeezing out the sample as in the standard sample containers. Wax samples were prepared using a clean cork borer of the same diameter as the sample pan. Wax was extruded from the cork borer and sliced with a razor blade into discs of the desired thickness. Petrolatum samples were prepared by melting a small quantity and placing the specimen in the sample pan with a glass capillary tube. Sample sizes ranged from 5 to 12 mg. The waxes and petrolatums were scanned at a rate of 10°C/min during normal cooling and heating runs. The first melting scans were not reported since they are often nonreproducible. This is probably due to a repositioning of the sample in the sealed pans.

Calibration

The calibration standards listed in Table 1 were run using similar instrumental conditions as the waxes. In some cases, it was necessary to reduce the sensitivity since the high purity of the standards gave large endothermic melting peaks. All of the standards were at least 99% pure. The temperature calibration was carried out using the extrapolated onset temperature of the melting peaks, T_m. The accuracy was considered sufficient for our work. A factor used for calculation of heat of fusion, ΔH_f, was determined from the area of the melting peak for pure indium. Six scans were made on three indium samples before a mean value was obtained.

TABLE 1

MELTING POINTS AND HEATS OF FUSION DETERMINED ON STANDARDS

	Lit. T_m *(°C)*	*Exp.* T_m *(°C)*	*Dev. (°C)*	*Lit.* ΔH_f *(cal/g)*	*Exp.* ΔH_f *(cal/g)*	*Dev. (%)*
n-Decane	−29.7	−28.5	1.2	48.3	47.8	1.0
Dist. water	0.0	2.0	2.0	79.7	80.6	1.1
n-Octadecane	28.2	30.5	2.3	57.6	55.8	3.1
Stearic acid	69.0	71.0	2.0	47.5	50.0	5.3
Naphthalene	80.2	79.0	1.2	35.1	33.0	6.0
Benzoic acid	122.4	121.5	0.9	33.9	34.9	2.9
Average deviation			1.7			2.8

RESULTS AND DISCUSSION

Melting scans

Figure 1 shows melting curves of two commercial paraffin waxes. The lower curve shows a solid–solid transition around 35°C and a peak melting point at 55°C. Solid–solid transitions have been discussed extensively in the literature[1, 4, 9]. Briefly, the transition is an orthorhombic to hexagonal crystalline rearrangement involving a rotational motion at the molecular level. From a practical aspect, the transition is important since a substantial amount of latent heat is involved. The upper curve in Fig. 1 was produced by a slightly lower melting wax and shows two solid–solid transitions. Barmby et al.[1] noted that only the low melting waxes have two transitions.

The total endothermic transitions, from onset of the solid–solid transition to completion of melting, generally occurred over temperature ranges of 40°C or more. Since petroleum waxes are mixtures of paraffinic compounds, as shown by the carbon number distribution in Fig. 2, overlapping of the solid–solid transitions and melting peaks is expected. Indeed, even at a scan rate of 2.5°C/min, the two peaks did not separate enough for the trace to return to the baseline. The primary melting peaks taken by themselves involve a relatively narrow temperature range as can be seen from the peak width at one-half the peak height.

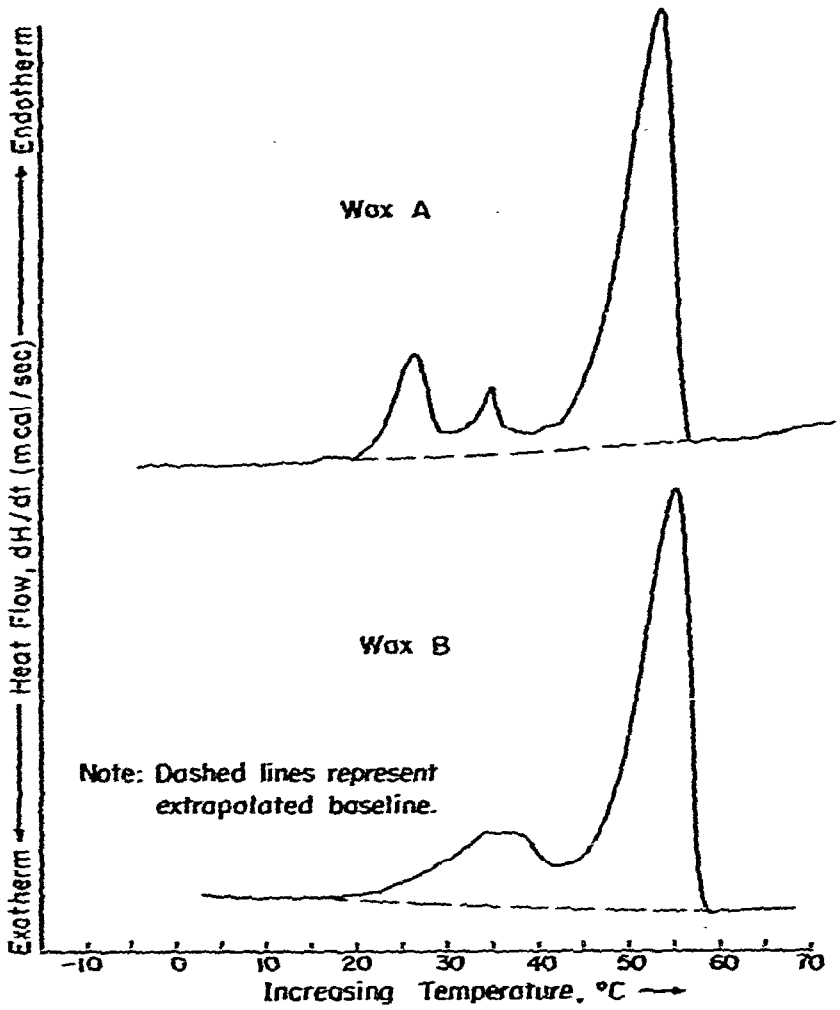

Fig. 1. DSC melting curves of paraffin waxes. Temperature program rate 10°C/min.

The melting curves of the petrolatums shown in Fig. 3 provide a contrast to paraffin waxes. Melting occurs over a wide temperature range with a single broad peak. Petrolatum begins melting at lower temperatures than paraffin wax and reaches a maximum endotherm around room temperature. The reason why petrolatum melts at lower temperatures, despite a higher molecular weight compared with paraffin waxes, involves at least two factors. The waxes in petrolatum are branched and cyclic paraffins* as opposed to normal paraffins which have higher melting points. In addition, petrolatum has a large oil fraction inherent in its composition. This oil has a solvent effect so that dissolution occurs at a temperature lower than isolated wax would ordinarily melt.

The upper two scans in Fig. 3 represent raw petrolatum stocks while the lower scan is that of a pharmaceutical grade petrolatum. The increased noise level in the

* Described in the trade as "microwaxes".

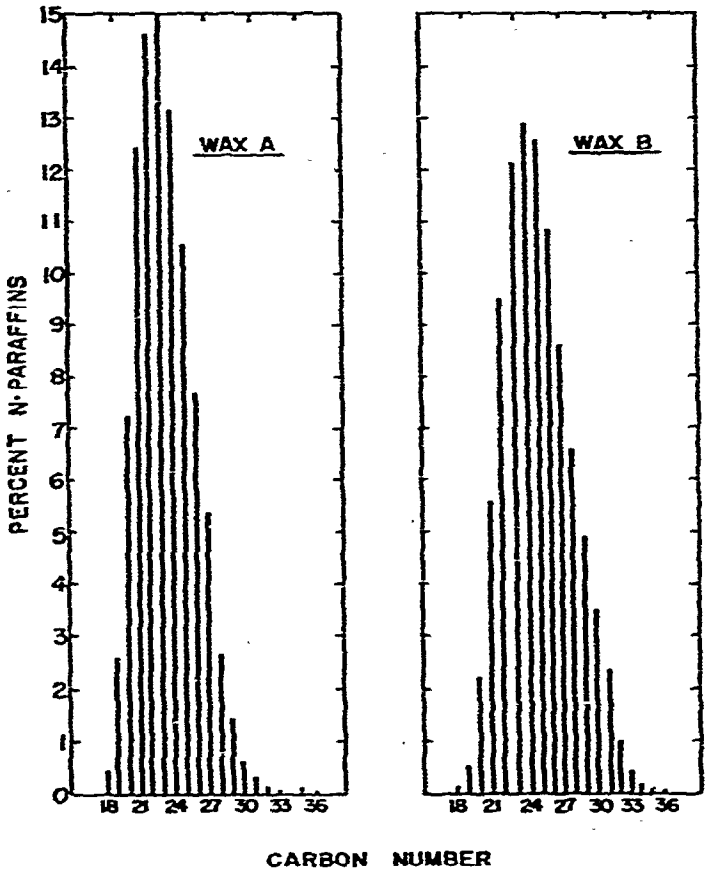

Fig. 2. Carbon number distribution of N-paraffins in waxes. (Gas chromatographic analysis neglects the iso- and cyclic-paraffins in waxes.)

petrolatum scans is due to the higher sensitivity at which petrolatum must be run compared with waxes. The higher sensitivity also increased baseline curvature which made onset and completion temperatures difficult to determine in some cases. The onset temperatures in Fig. 3, for example, were chosen by "eyeballing" the extrapolated baseline. The baseline displacement of Stock A between −70 and −56°C is interpreted as a glass transition. With the large amorphous oil fraction in petrolatum, one would expect to find glass transitions more frequently than we have. It is possible that the glass transition for some samples is at lower temperatures than our work involves.

The onset of the endothermic peak is considerably below room temperature for both wax and petrolatum. In the case of waxes, this means a certain amount of rotational motion is occurring at room temperature. In the case of petrolatum, approximately half of the crystallizable compounds are already melted. The result in both materials is a softer product than at subambient temperatures. The semi-solid nature of petrolatum at room temperature can then be attributed to three factors in its composition: Inherent oil, a fraction of melted microcrystalline wax, and solid microcrystalline wax.

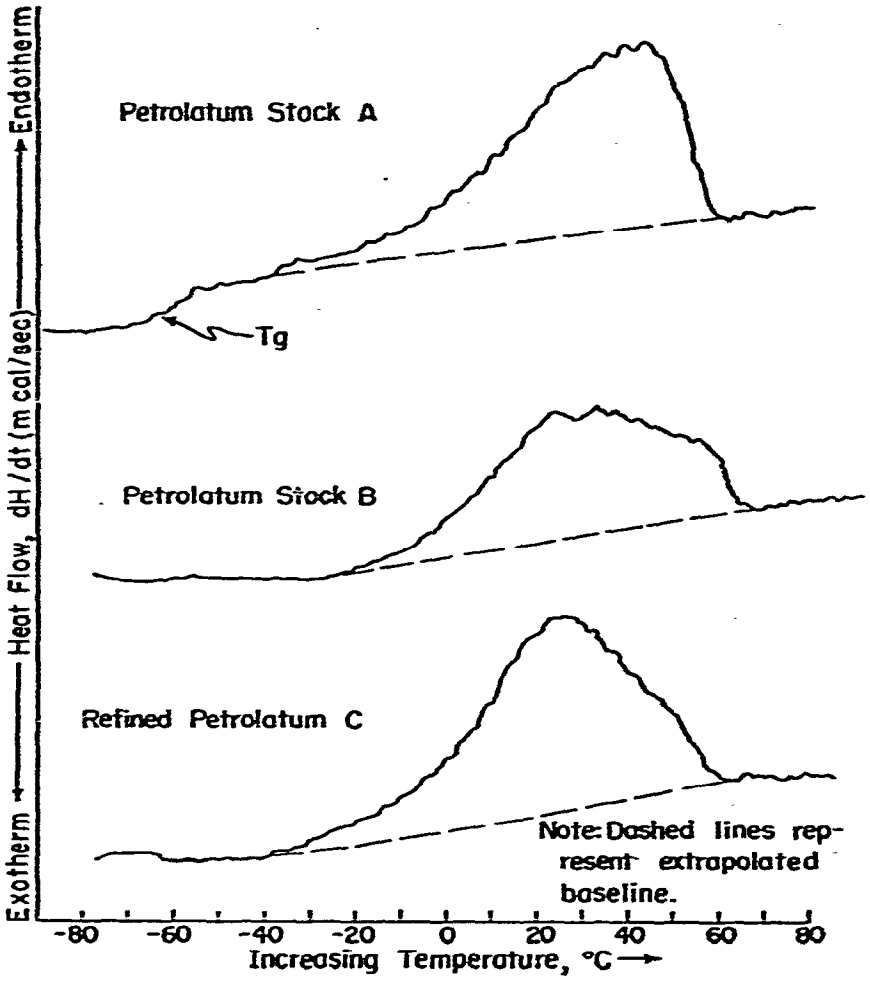

Fig. 3. DSC melting curves of petrolatums. Temperature program rate 10°C/min.

Crystallization scans

The preceding discussion was limited to melting phenomenon obtained from DSC heating scans. Figure 4 shows exothermic crystallization peaks obtained using the same samples as in Fig. 1. The crystallization peaks are essentially mirror images of the melting peaks except that the cooling curves were shifted to slightly lower temperatures. That is, crystallization (during cooling at 10°C/min) occurs at temperatures 5–8 degrees lower than the melting scans (during heating at 10°C/min).

The petrolatum crystallization scans are shown in Fig. 5. In the case of petrolatum, the initial crystallization from the liquid often results in a sharp spike. This is demonstrated by Scans B and C in Fig. 5. This initial exotherm is probably caused by the crystallization of a small fraction of normal paraffins which may be present in petrolatum.

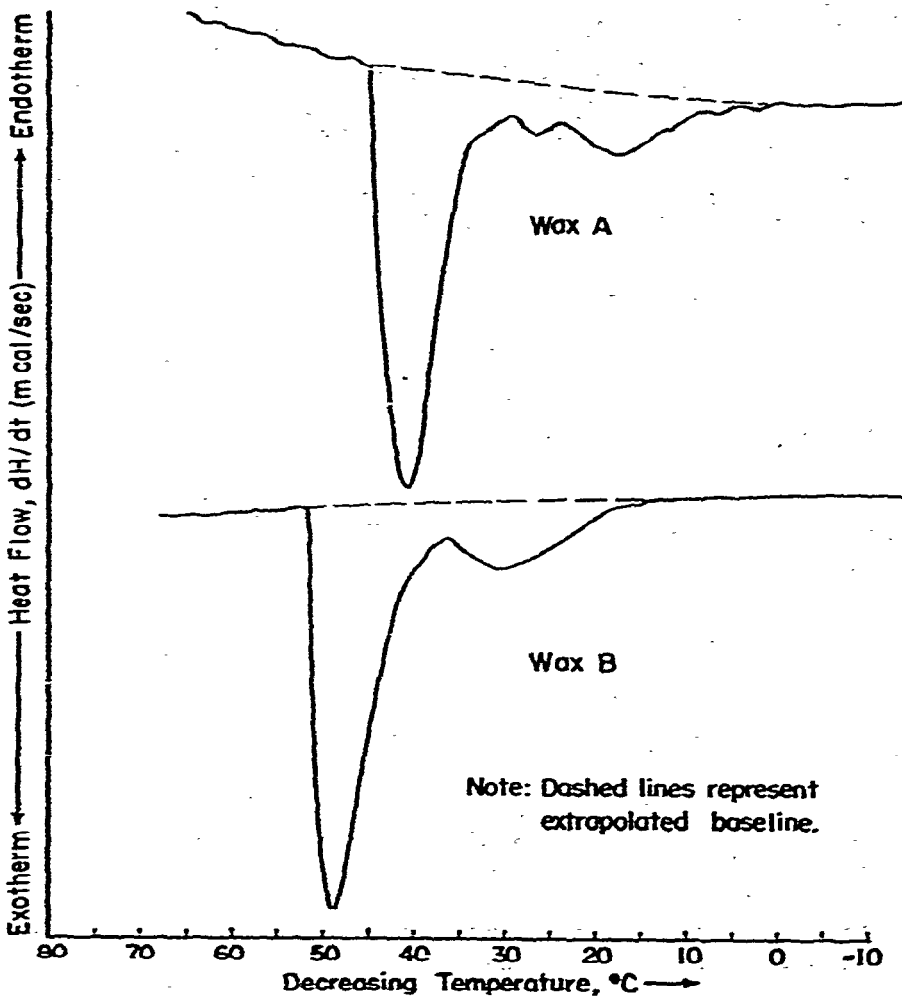

Fig. 4. DSC crystallization curves of paraffin waxes. Cooling rate 10°C/min.

Effect of temperature program rate

The effects of various temperature program rates on melting and crystallization phenomenon are conveniently studied by DSC. Melting curves of four paraffin waxes were obtained at heating rates of 2.5, 5, 10, 20, and 40°C/min. A common cooling rate of 10°C/min was used between each melting scan. The same samples were then programmed at various cooling rates to obtain crystallization scans.

The results of the various temperature program rates for two of the waxes are shown in Table 2. As expected, there is a significant effect on the peak temperatures caused by the thermal resistance between the sample and its platform (temperature sensor). The greater the temperature program rate, the greater will be the displacement from equilibrium conditions. In essence, at fast program rates, the sample temperature cannot keep pace with the platform temperature.

The experimental peak temperatures in Table 2 were fitted to three term regression equations and plotted in Fig. 6. The parabolic equations for each curve are

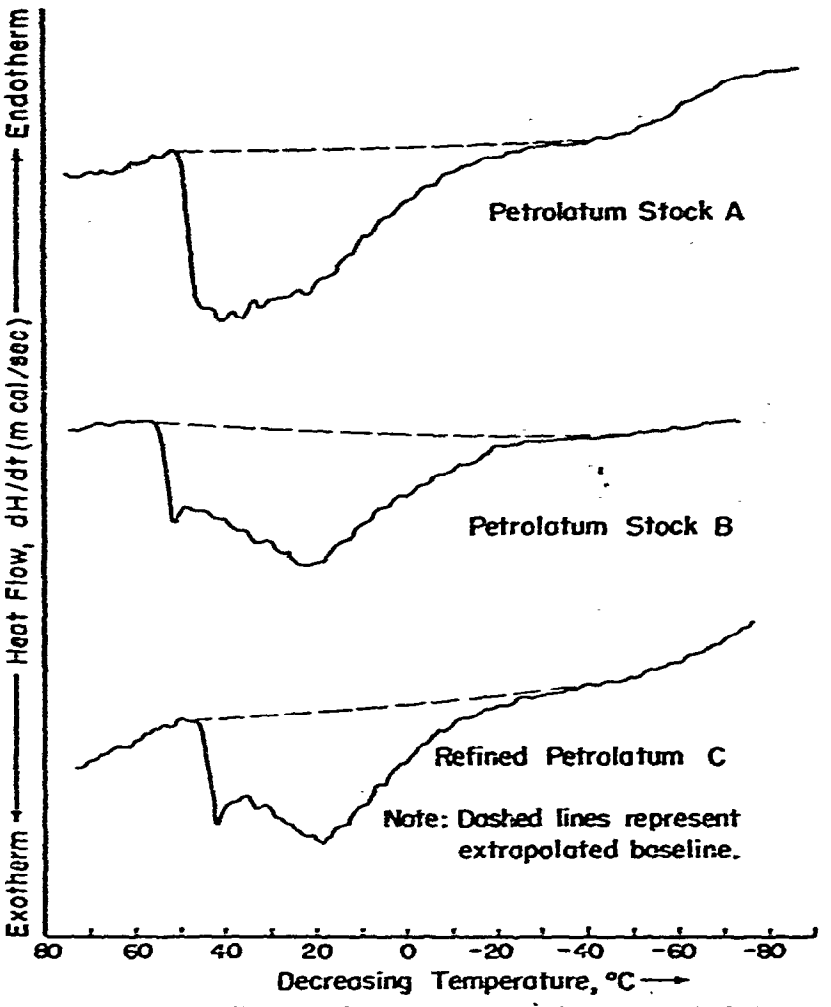

Fig. 5. DSC crystallization of petrolatums. Cooling rate 10°C/min.

TABLE 2

THE EFFECT OF VARIOUS TEMPERATURE SCAN RATES ON MELTING AND CRYSTALLIZATION OF PARAFFIN WAXES

Sample	*Temp. program rate (°C/min)*	*Peak temperature (°C)*	
		Melt scan	*Cryst. scan*
Wax A	2.5	51	46.5
(m.p. 46°C)[a]	5	52	44
	10	54	41.5
	20	58	37
	40	63.5	30
Wax B	2.5	53	51
(m.p. 52°C)[a]	5	53.5	50
	10	55	48
	20	57	45
	40	61	40

[a] Measured by ASTM D-87 melting point of petroleum wax (cooling curve).

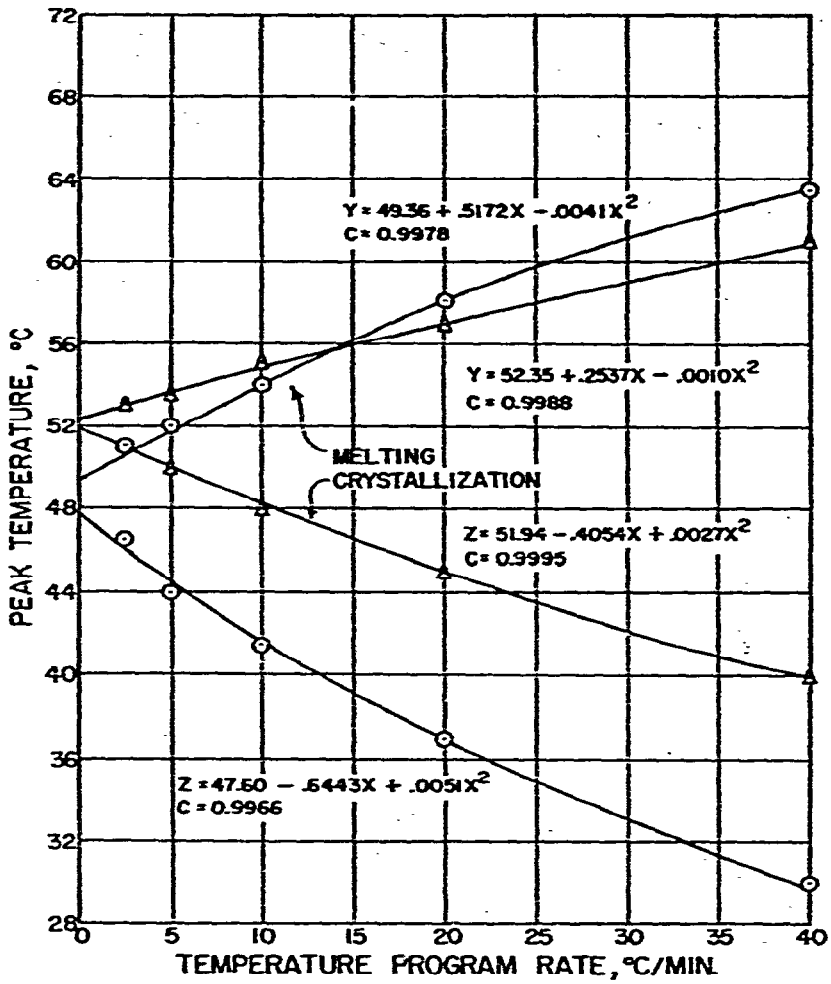

Fig. 6. Effect of scan rate on DSC peak temperatures of paraffin waxes. ⊙, Wax A; △, Wax B.

given in Fig. 6 along with their correlation coefficients, C. The correlation coefficients indicate good fits for all of the equations.

The question arises as to why a standard temperature rate of 10°C/min was used when a slower rate would be more accurate in terms of an equilibrium melting point. The scan rate was chosen partly for convenience but also because it gave larger peaks than at slower rates. DSC scans of petrolatum are especially difficult at slower scan rates since the endotherms are relatively small and cover a wide temperature range. An additional argument for using a scan rate of 10°C/min is the adoption of that rate in two new ASTM Standards[10, 11]. In practical terms, waxes and petrolatum are seldom heated under ideal conditions. A 55-gal. drum of wax, for example, may heat quickly around the outer walls, but very slowly in the interior.

DSC versus traditional melting points

The obvious advantage of thermal analysis over traditional melting point methods is that the entire melting or crystallization curve is observed. Details of

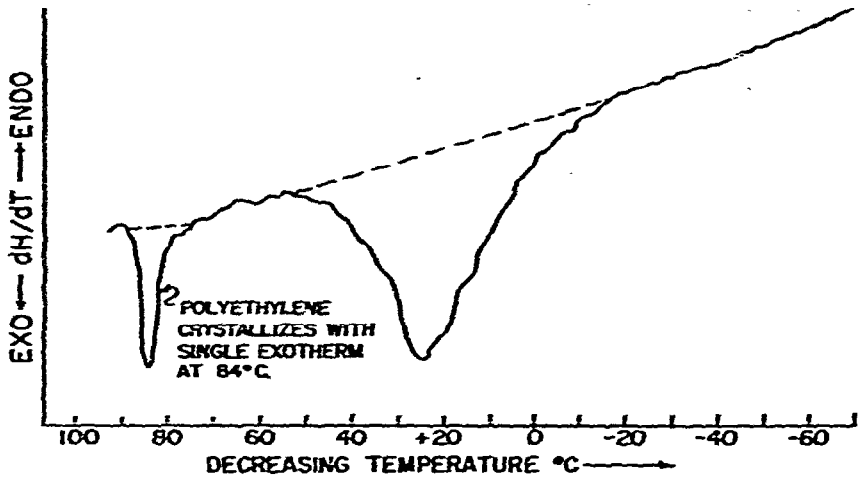

Fig. 7. DSC cooling curve of petrolatum–polyethylene blend. Cooling rate 10°C/min.

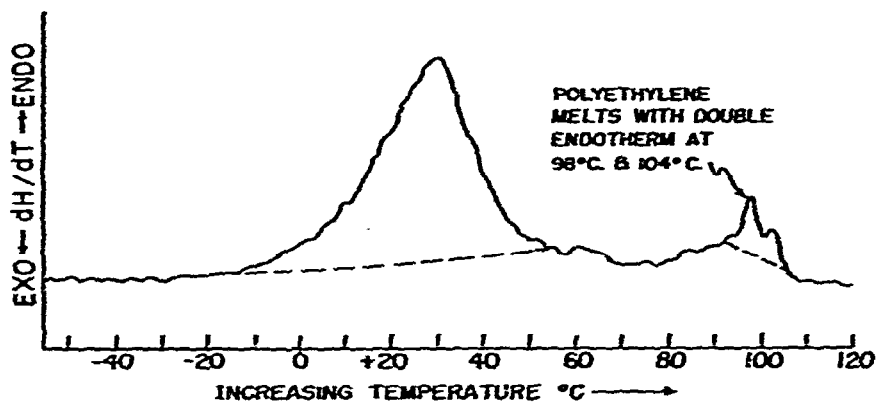

Fig. 8. DSC melting curve of petrolatum–polyethylene blend. Heating rate 10°C/min.

such scans were discussed earlier. Another illustration of the advantage of a complete scan is shown in Figs. 7 and 8. The curves show the melting and crystallization of a petrolatum (92%)–polyethylene (8%) blend. The entire petrolatum melting peak is complete around 55°C while the polyethylene melts with a double peak at 98 and 104°C. When the usual ASTM petrolatum melting point procedure[12] was applied to such a product, the result was a misleadingly high value of 93°C.

The ASTM melting points for unblended petrolatums were found to have no relation to their DSC scans. This was expected since the ASTM melting point for petrolatum is arbitrarily defined as that temperature at which a drop falls from the bulb of a thermometer when heated at a prescribed rate. This method depends on rheological properties as well as on actual melting[13].

The relationship of DSC data to the ASTM cooling curve melting point[14] of paraffin waxes was also investigated. For this correlation, it is necessary to go back to the peak temperature versus scan rate curves in Fig. 6. The most interesting feature of the plots is that the melting and cooling curves for a particular wax extrapolate to

nearly the same temperature at zero heating or cooling rate. The extrapolated temperatures were found to correspond, within a few degrees centigrade, to the ASTM cooling curve melting points for the waxes.

The basis for the cooling curve melting point is that wax gives up its heat of fusion at the melting point. Therefore, the rate of cooling levels off at the melting point. Since the ASTM method obeys Newton's Law of Cooling*, the sample cools at an exponential rate which is very slow near the melting point. The ASTM method approaches the melting point at nearly equilibrium conditions. This contrasts with the DSC which controls heating and cooling at a linear rate. DSC peak temperatures converge upon the ASTM melting point only when very slow temperature program rates are used.

Heats of fusion and crystallinity

Table 3 gives the heats of fusion of four paraffin waxes determined by DSC. The areas measured by a planimeter included the total endotherms for the melting scans. Each datum in Table 3 represents an individually weighed specimen and the average of at least two planimeter measurements. Pooling the variances gave a standard deviation of 1.44 cal/g for all of the data. The main source of error was probably the extrapolation of the baseline, particularly at the onset temperature. Since the solid–solid transitions did not return to the extrapolated baselines, only estimates of the heats of transition were made. A perpendicular was dropped from the minimum between peaks, to the extrapolated baseline. This technique gave an estimated ΔH for the solid–solid transitions of 5.4 and 2.9 cal/g for Wax A and 10.8 cal/g for Wax B. The heats of fusion for the actual melting of Wax A and Wax B were estimated to be 35.2 and 32.1 cal/g, respectively. No attempt was made to replicate heats of fusion for petrolatum samples. Single determinations for the petrolatum scans in Fig. 3 were 12.0 and 20.2 cal/g for Stocks A and B, respectively and 15.6 cal/g for the refined petrolatum, C.

TABLE 3

HEATS OF FUSION OF PARAFFIN WAXES DETERMINED BY DSC

Scan no.	*Heats of fusion, ΔH_f (cal/g)*			
	Wax A	*Wax B*	*Wax C*	*Wax D*
1	43.9	44.4	41.7	41.7
2	44.2	41.7	43.9	41.7
3	42.3	42.7	43.8	45.1
Mean	43.5	42.9	43.1	42.8
Standard deviation, S	1.04	1.36	1.24	1.96
Variance, S^2	1.02	1.86	1.54	3.85

Pooled precision for all data above is $S_p = 1.44$ and $S_p^2 = 2.07$.

* Newton's Law: $dx/dt = a(x - T_s)$, where x = temperature at any time, t; T_s = temperature of surroundings; a = constant. Integrated form: $x = ce^{at} + T_s$.

TABLE 4

THEORETICAL HEAT OF FUSION, ΔH_f^{*a}, OF WAX A CALCULATED FROM CARBON NUMBER DISTRIBUTION OF N-PARAFFINS

Carbon no.	*Wt.%*	*Lit. ΔH_f^{*b} (cal/g)*	*$\Delta H_f \times$ wt.%/100*
18	0.45	57.64	0.259
19	2.60	53.07	1.380
20	7.23	59.10	4.273
21	12.43	50.91	6.328
22	14.63	59.37	8.686
23	15.09	55.75	8.413
24	13.18	60.83	8.017
25	10.56	56.79	5.997
26	7.67	59.77	4.584
27	5.39	56.10	3.024
28	2.69	60.59	1.630
29	1.42	56.02	0.795
30	0.65	59.40	0.386
31	0.34	57.68	0.196
32	0.14	58.70	0.082
			$\Delta H_f^* = \Sigma =$ 54.04 cal/g

[a] ΔH_f^* includes heats of transitions as well as heats of fusion.
[b] From ref. 17.

The heats of fusion for the total endotherms given in Table 3 are valid for making engineering calculations. For example, the ΔH_f's can be used along with heat capacity to calculate the total amount of energy required to melt a given quantity of wax. There are, however, limitations to the use of the data in Table 3.

Waxes are not 100% crystalline materials. In fact, they contain a certain portion of amorphous compounds which are primarily cyclic and isoparaffins. Since the experimental ΔH_f's were based on the total specimen weight, including the amorphous material, the experimental ΔH_f is lower than the theoretical ΔH_f° for 100% crystalline material.

Polymer chemists take advantage of the crystalline–amorphous concept of semi-crystalline polymers in order to calculate the degree of crystallinity, $\Delta H_f/\Delta H_f^\circ$, of polymers[15, 16]. The same calculation (crystallinity = $\Delta H_f/\Delta H_f^\circ$) can be applied to waxes. In the case of polymers, ΔH_f° is not easily obtained. However, in the case of waxes, it can be calculated from the carbon number distribution and literature values for the pure compounds. Table 4 illustrates the calculation of ΔH_f° for Wax A. Since literature values for the combined heats of transition and heats of fusion were available[17], they were used with the mean experimental ΔH_f values from Table 3. Applying the equation above gives a crystallinity of 0.80 for Wax A and 0.78 for Wax B.

The significance of crystallinity measurements is similar to that in polymers[18]. Wax can be thought of as a two-phase system consisting of a crystalline fraction X,

which is the crystallinity determined above, and an amorphous fraction, $1 - X$. Many of the bulk properties of a wax such as density, refractive index and heat capacity are simply combinations of these properties from the two phases.

The calculation of crystallinity cannot be applied to petrolatum since a complete gas chromatographic analysis of high molecular weight fractions is not possible. Only an estimate could be made based on an analogy to wax. Since heats of fusion for petrolatum are usually less than one-half of those for waxes, we would expect a crystallinity of less than 0.40 for petrolatum. However, since approximately one-half of the crystalline material in petrolatum is melted at room temperature, the crystallinity would drop to approximately 0.20 or less. This is another indication of the semi-solid nature of petrolatums.

Specific heat and enthalpy

The DSC scans described earlier do not have their ordinates calibrated in actual units. The vertical axis can be converted to enthalpy and specific heat if the true baseline of a scan is available. The true baseline is obtained by running a scan with an empty pan before the sample is run in the same pan. Quantitative measurements of heat effects by DSC are usually derived from areas. By measuring the amplitudes at one-degree intervals, it is possible to divide a scan into narrow trapezoidal areas and compute the enthalpy per degree[18]. Since enthalpy per degree defines specific heat,

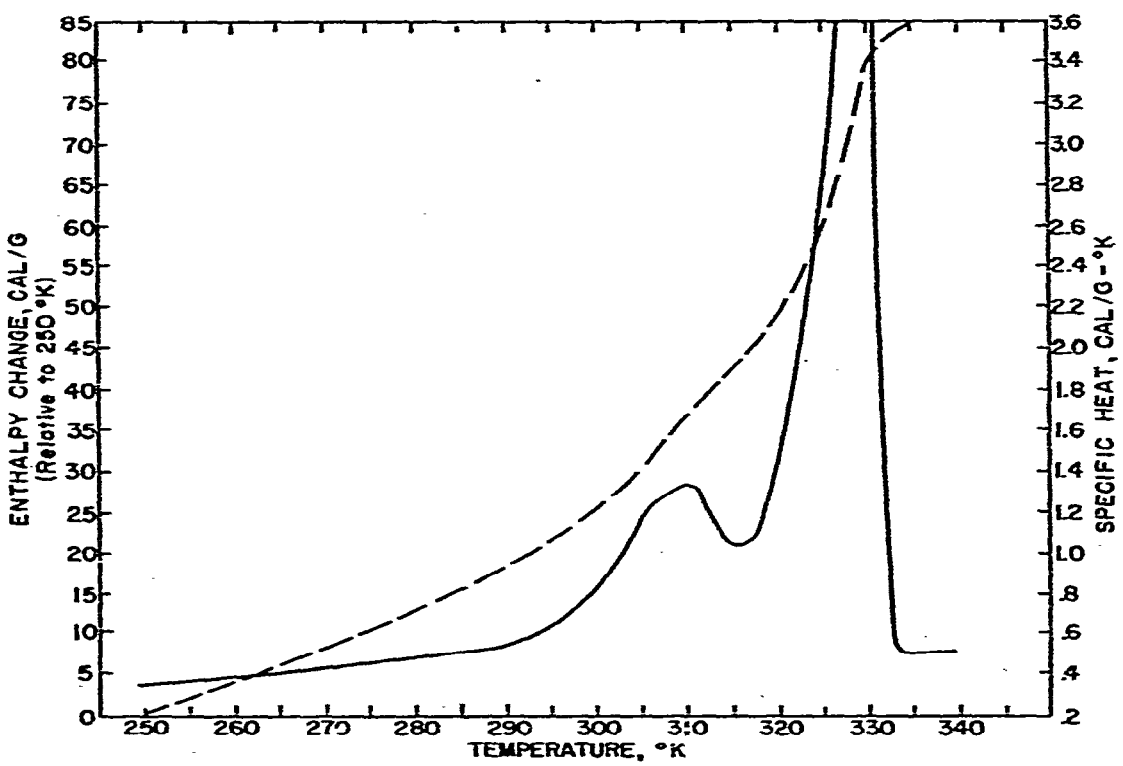

Fig. 9. Enthalpy (----) and specific heat (——) of Wax B derived from DSC scans.

a record is produced which records specific heat as a function of temperature. By continuously summing the enthalpy units, the change in enthalpy is recorded relative to the arbitrary starting point.

Perkin-Elmer has instrumentation available that performs the functions described above automatically. In our case, the amplitudes were measured by hand and the computations were performed by computer. Figure 9 shows the resulting plots of enthalpy relative to 250 K and specific heat for Wax B. It can be seen that the computed specific heat curve is the same shape as a DSC curve obtained directly from the instrument. The enthalpy curve gives the total amount of energy required to bring one gram of Wax B from 250 K to any other temperature up to 340 K. The enthalpy between any two temperatures in this range can be obtained simply by subtracting the lower value from the higher value.

The enthalpy curve in Fig. 9 can be used by engineers to determine the most efficient temperature range for the storage of solar energy. The steepest part of the curve is coincident with the melting peak between 323 and 332 K. The enthalpy in this relatively narrow, nine-degree temperature range is 28.5 cal/g. If a wider temperature range is acceptable, the total endothermic peaks can be used between 289 and 334 K. This temperature range would allow the storage of 65 cal/g of solar energy in Wax B.

The strict definition of specific heat for pure compounds excludes its measurement at temperatures where first-order transitions take place. Indeed, specific heat is infinite at such temperatures. However, as demonstrated in Fig. 9, specific heat can be recorded while a transition or melting peak is occurring in real mixtures of organic compounds. The reader should understand that the specific heats shown for Wax B involve contributions from first-order transitions as well as from sensible heat. To record sensible heats without interference from endothermic transitions, temperatures must be less than the onset of the solid–solid transition or greater than the completion of melting. Another method of measuring specific heat was used in these ranges.

TABLE 5

SPECIFIC HEAT OF WAX B

	Temperature (°C)	*Specific heat (cal/g °C)*	
		Sapphire as standard	*From Fig. 9*
Solid	−20	0.381	0.365
	−15	0.399	0.385
	−10	0.403	0.405
	− 5	0.424	0.425
	0	0.428	0.458
	5	0.455	0.478
Liquid	85	0.578	
	90	0.580	
	95	0.581	
	100	0.585	
	105	0.590	

Perkin-Elmer recommends a specific heat method that uses sapphire as a standard[19]. This method was tested on pure naphthalene and found to agree with the literature to ±5%. The sapphire procedure was used to make the specific heat determinations in Table 5. Data from Fig. 9 are included for comparison of the methods. The sapphire method is preferred because of its greater accuracy, but it is more time consuming since individual scans can only cover 20–30 degrees at a time.

CONCLUSIONS

Complete DSC scans of waxes and petrolatums can be made when auxiliary cooling is used. Even though thermal equilibrium is not ordinarily achieved, the scans provide useful information to characterize the crystalline phase of waxes and petrolatums. Quantitative measurements of basic thermodynamic data provide information on the energy requirements of a wax from subambient temperatures to temperatures above the melting point.

ACKNOWLEDGMENTS

The author wishes to thank Dr. F. Noel of Imperial Oil Enterprises and Dr. W. P. Brennan of Perkin-Elmer for several helpful suggestions.

GLOSSARY

T_m	Extrapolated onset temperature. Used for pure compounds only.
ΔH_f	Heat of fusion plus heats of transition (if present) determined by DSC.
ΔH_f°	Heat of fusion plus heats of transition (if present) of 100% crystalline material.
T_g	Glass transition temperature.
X	Weight fraction of crystalline material.
$1 - X$	Weight fraction of amorphous material.

REFERENCES

1 D. S. Barmby, L. G. Bostwick and J. A. Huston, Jr., *Proc. 6th World Pet. Congr.*, 1963, Sect. VI, p. 161.
2 B. R. Currell and B. Robinson, *Talanta*, 14 (1967) 421.
3 R. G. Craig, J. M. Powers and F. A. Peyton, *J. Dent. Res.*, 46 (1967) 1090.
4 R. G. Craig, J. M. Powers and F. A. Peyton, *Anal. Calorimetry, Proc. 155th Am. Chem. Soc. Symp.*, 1968, p. 157.
5 B. Flaherty, *J. Appl. Chem. Biotechnol.*, 21 (1971) 144.
6 C. Savu, C. Giavarini and F. Pochetti, *Pet. Gaze*, 21 (1970) 117.
7 C. Giavarini and F. Pochetti, *J. Therm. Anal.*, 5 (1973) 83.
8 F. Noel, *Thermochim. Acta*, 4 (1972) 377.
9 R. T. Edwards, *Tappi*, 41 (1958) 267.
10 *1976 Annual Book of ASTM Standards, Part 35*, D 3417-75, ASTM, Philadelphia, 1976.
11 *1976 Annual Book of ASTM Standards, Part 35*, D 3418-75, ASTM, Philadelphia, 1976.

12 *1976 Annual Book of ASTM Standards, Part 23*, D 127-63, ASTM, Philadelphia, 1976.
13 A. Kinsel and J. Phillips, *Drug Cosmet. Ind.*, 67 (1950) 628.
14 *1976 Annual Book of ASTM Standards, Part 23*, D 87-74, ASTM, Philadelphia, 1976.
15 P. J. Flory, *Principles of Polymer Chemistry*, Cornell University Press, Ithaca and London, 1953, p. 573.
16 M. Dole, *J. Polym. Sci., Part C, Polym. Symp.*, 18 (1967) 57.
17 F. W. Billmeyer, Jr., *J. Appl. Phys.*, 28 (1957) 1114.
18 A. P. Gray, *Thermochim. Acta*, 1 (1970) 563.
19 *Instructions, Specific Heat Kit*, 219-0136, Perkin-Elmer, Norwalk, 1968.